



PERGAMON

Engineering Failure Analysis 10 (2003) 85–91

**ENGINEERING  
FAILURE  
ANALYSIS**

www.elsevier.com/locate/engfailanal

## Turbine blade failure in a thermal power plant

Goutam Das\*, Sandip Ghosh Chowdhury, Ashok Kumar Ray,  
Swapan Kumar Das, Deepak Kumar Bhattacharya

*Materials Characterisation Division, National Metallurgical Laboratory (CSIR), Jamshedpur-831007, India*

Received 12 March 2002; accepted 12 May 2002

---

### Abstract

The failure of a LP (low pressure) turbine blade of a 220 MW thermal power plant is presented. The blade was made of martensitic stainless steel and the structure was tempered martensite. There was no evidence of degradation of blade material. The fracture took place at the aerofoil region, 113-mm from the root. Throughout the blade surface Si rich phases were detected. Several pits/grooves were found on the edges of the blades and chloride was detected in these pits. These were responsible for the crevice type corrosion. The probable carriers of  $\text{Cl}^-$  were Ca and K, which were found on the blade. The failure mode was intergranular type. Possibly the ultimate failure was due to corrosion-fatigue. © 2002 Elsevier Science Ltd. All rights reserved.

*Keywords:* Turbine blade; Corrosion fatigue; Failure analysis; Fractography; Intergranular fracture

---

### 1. Introduction

In recent times, LP blades of a steam turbine are generally found to be more susceptible to failure than IP (intermediate pressure) and HP (high pressure) blades. Among the various blade materials the most popular is 12% chromium martensitic steel. It has an excellent combination of strength, toughness and corrosion resistance as well as high inherent damping characteristics [1–3].

The present paper reports the investigation of the failure of a blade in the LP stage of a thermal power plant of 220 MW capacity. The unit was shut down because of noise in the turbine assembly. After opening the turbine casing, one blade in the LP region was found fractured. The blade before fracture had completed 33,000 h of service. The blade which had failed was from the 29th stage. This stage has 120 blades. Thus, there are 15 such buckets. Bucket 8 contained the fractured blade (blade no 61). The fracture took place at the aerofoil region, 113-mm from the root. The fractured blade was number 4 in that bucket. The other blade, which did not fail but completed the same number of cycles, was the 5th from the same bucket. The lacing rods connecting the other blades i.e. 3rd to 6th were also found to be broken, however, the remaining portion of the lacing rods on both ends remained intact. These failures were presumably a result of impact by the broken piece of the blade mentioned earlier. The objective of the investigation was

---

\* Corresponding author. Tel.: +91-657-271-710; fax: +91-657-270-527.

E-mail address: asokroy@nmlindia.org (G. Das).

to identify the root cause of failure and to ascertain whether it was due to a materials related problem or due to changes in operational parameters arising from the grid frequency, boiler water chemistry etc. Investigation was also conducted on a blade nearby the fractured blade and also on a blade which had completed 100,000 h of operating period.

## 2. Experimental procedure

Chemical analysis of the blade material was carried out by a standard wet method. A portion of the failed blade with the fracture surface was cut for fractography study. A portion of the fractured blade (100 mm away from the fracture surface, as shown in Fig. 1) was cut for metallography. A few random pieces were also cut from the other two blades as already mentioned (i.e. 33,000 h service exposed and 100,000 h service exposed) for SEM and metallography. The metallography samples were prepared by using standard metallographic techniques and etched with Glycergia (a dilute solution of HCl, HNO<sub>3</sub> and glycerol). The microstructure of the blade material was analysed by optical microscope and a JEOL-840 scanning electron microscope (SEM) equipped with an energy dispersive X-ray (EDX) analysis facility. Hardness values were measured using a Vickers Hardness Testing machine under 10-kg load.

## 3. Results

### 3.1. Visual inspection

The fractured surface of the blade, which failed in the first place, revealed a smooth surface. Beach marks were observed and indicated that the crack might have originated from the thinner side of the blade. Some portion of the fractured surface appeared black which is indicative of the presence of Fe<sub>3</sub>O<sub>4</sub> (magnetic) scale. The blade revealed the presence of adherent scale of varying thickness.

### 3.2. Chemical analysis

The blade material was found to have the following material composition: C-0.21; Si-0.51; Mn-0.43; Cr-13.64; Mo-0.22; Ni = 0.51; balance-Fe. This material conforms to ASTM 410 grade martensitic stainless steel.

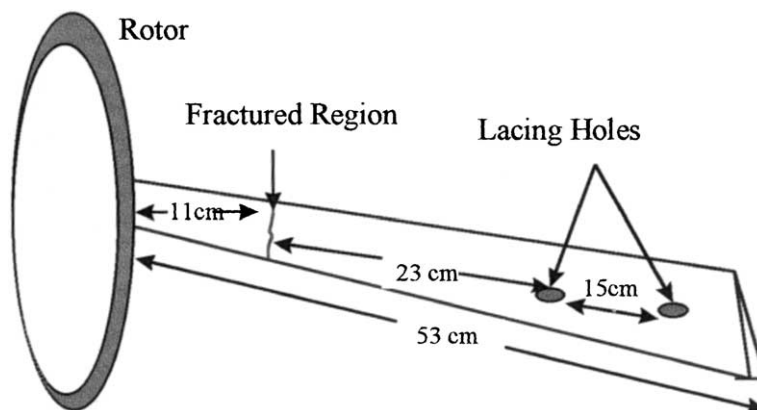


Fig. 1. Schematic of the turbine blade with the fractured region as shown.

### 3.3. Microstructure

SEM micrography shows a tempered martensitic microstructure [Fig. 2(a)]. Micrographs of the other two blades also show a similar microstructure [Fig. 2(b)]. Similar features were observed in randomly selected specimens indicating homogeneity of microstructure. There was no evidence of microstructural degradation in the failed blade or in the one which did not fail. This is expected because the temperature that the blades were exposed to was low (of the order of 150 °C).

Several grooves were observed along the blade edges [Fig. 3(a)]. These grooves are parallel to the fracture surface and several such grooves were present throughout the blade edges. However, compared to the fractured blade, the density of the grooves was less in the other blade. EDX analysis revealed the presence of substantial amount of Si in the grooves [Fig. 3(b)].

Observation of the blade edges (33,000 h service exposure) of the nearby failed blade showed a Si-rich phase within the material [Fig. 4(a)] which is confirmed from Fig. 4b. There were some fine cracks which had been exposed to the ambient temperature.

### 3.4. Fractography

The low magnification image of the fractured surface of the failed blade is shown in Fig. 5. Several beachmarks can be seen on the fracture surface. The curvature of the beachmarks indicates that the crack

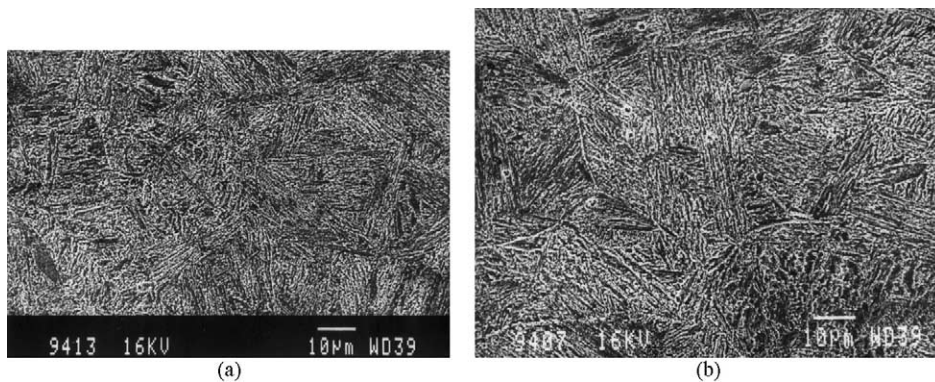


Fig. 2. SEM micrographs of (a) fractured blade and (b) nearby blade. Tempered martensite is clearly revealed from both the microstructures.

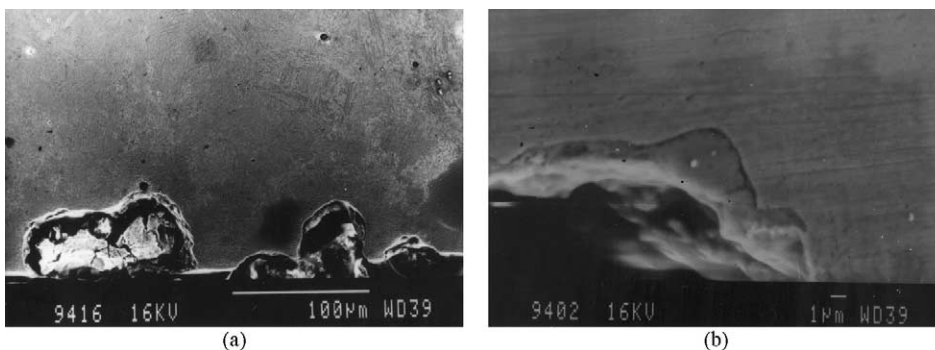


Fig. 3. Fractographs of the fractured blade (a) showing several grooves along the blade edges and (b) indicating the presence of a substantial amount of Si in the grooves.

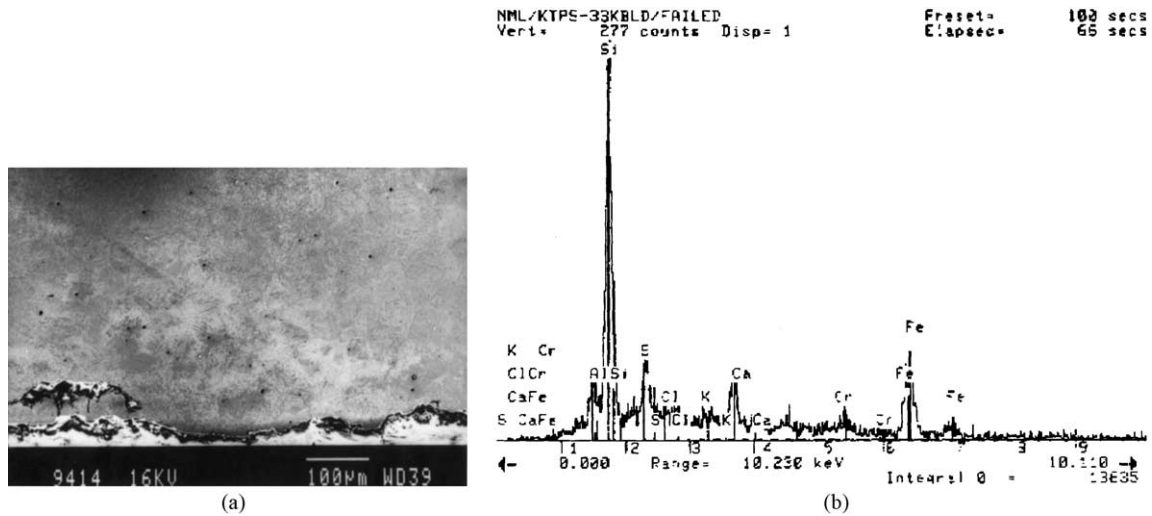


Fig. 4. (a) SEM micrograph showing Si rich phases in the grooves and (b) SEM-EDX confirming the presence of Si.

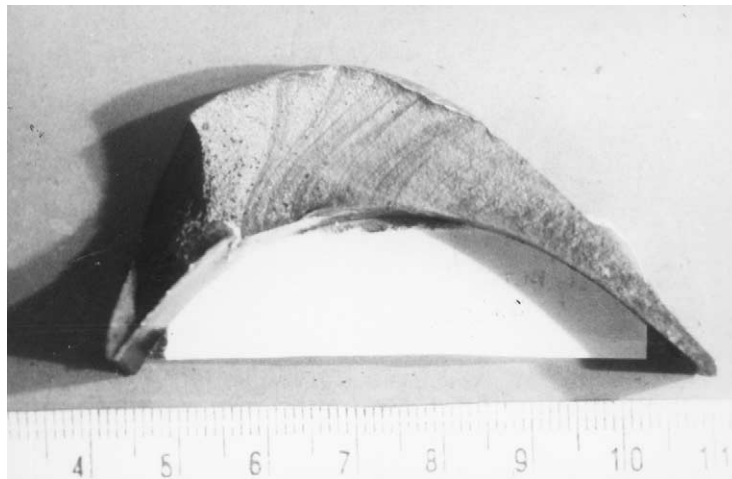


Fig. 5. Micrograph of the fractured blade, showing several beachmarks and also the crack initiation point, which is towards the thinner side of the blade.

initiation point is towards the thinner side of the blade. The SEM fractography showed intergranular fracture mode at the starting point [Fig. 6(a)]. This morphology was observed till final fracture [Fig. 6(b)]. In a few areas, cleavage type fracture mode was also observed. The presence of beachmarks along with the intergranular morphology of the fracture surface indicates that corrosion fatigue could play a strong role in controlling the initiation as well as propagation of the crack. The possibility of corrosion due to steam is not ruled out. The fracture surface also showed pits of shallow depth, which might have been generated after the initiation of the crack (Fig. 7). The pits were observed very near to the blade edge. SEM-EDX indicates the presence of chloride ions inside the pits. These pits were oriented perpendicular to the fracture surface and did not have any role in the fracture process. However, their presence indicates that a corrosion environment was available which caused pitting.

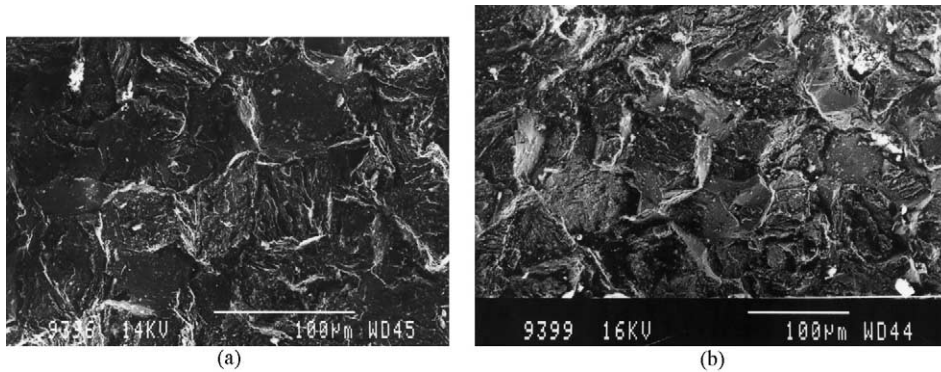


Fig. 6. (a and b) Fractured surface showing an intergranular type of fracture with a cleavage type fracture in few areas.

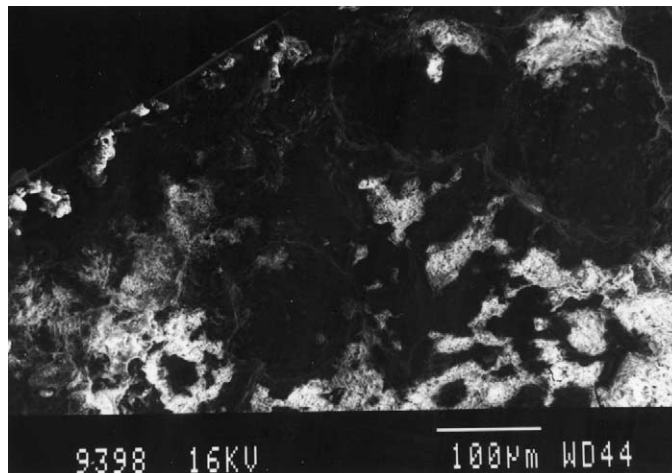


Fig. 7. SEM micrograph of the fractured surface showing several corrosion pits.

### 3.5. Hardness

Hardness of the materials was 248 VHN (RC 24) which is well within the recommended value for this grade of steel. The tensile stress in MPa was evaluated from VHN data by the following relation [4]:

$$\sigma_{TS}(\text{MPa}) = 3.2 \times \text{Hv}.$$

Therefore, the tensile stress was 794 MPa, which is the recommended value for this grade of steel.

## 4. Discussion

It is necessary to address the following points in order to analyse the failure of the LP turbine blade: (i) whether the material of the blade was defective; (ii) whether the operating conditions had any influence on the degradation and failure of the blades.

The material is as per the chemical composition and mechanical property values of martensitic stainless steel. There is neither inhomogeneity nor any microstructural degradation of the blade material. Therefore, the possibility of material failure due to material degradation is ruled out. This is of course, expected, since the material temperature was low.

There were several grooves at the edges of the blade. These grooves, in a few cases were found to be enriched with a Si phase. XRD analysis of the scale adherent to the blade surface indicated that it was SiO<sub>2</sub>. Normally the source of SiO<sub>2</sub> is steam. During rotation of the blade under steam pressure, these SiO<sub>2</sub> particles impinge on the blade material and form grooves by repeated strikes (erosion corrosion) [5,6]. The process of erosion by SiO<sub>2</sub> particles is dependent on the particle size, morphology as well as its velocity with which it strikes the blade material. If we consider the SiO<sub>2</sub> particles as spherical balls then the area in the matrix after material loss would look like a cone. The space behind the particle would act as a crevice and lead to crevice corrosion.

The pits observed on the fracture surface were found to contain chlorine, which facilitates initiation and propagation of crevice attack. The possible sources of Cl<sup>-</sup> are steam and feed water through a condenser tube due to leakage. The possible carriers of the chloride were Ca and K. They were found throughout the blade surface. From the beach marks on the fracture surface, it could be seen that the fracture initiation points lay at the aerofoil trail edge region, which has the thinnest cross-sectional area. Therefore, in this area a plane stress condition prevails. Under plain stress condition, fracture toughness is very much dependent on the specimen geometry. Therefore, formation of crevices below the SiO<sub>2</sub> particle on the blade surface would be the ideal position for crack initiation. Nevertheless, in a LP turbine, under the reduced load (in a load following plants) the so-called Wilson Line (point of initial condensation) shifts to a higher temperature point [7]. In cyclic operations the load fluctuates (i.e. decreases and increases) and so the blade surface is alternately getting wet and dry. As long as the steam is dry there is very little corrosion. But with little condensation the steam might contaminate with high concentration of chloride salt as steam condensate contains 10<sup>6</sup> times more salt than steam vapour [8,9]. Under reduced load this salt might deposit on the blade surface facilitating corrosion attack. Again, during shut down, O<sub>2</sub> and CO<sub>2</sub> might dissolve in the acidic salt (due to evaporation of NH<sub>3</sub>) and might aggravate the corrosive condition.

The yield strength of the material could be approximated from its UTS values (~800 MPa) and should be of the order of ~600 MPa [2]. Under normal operating conditions two major stresses act on the blade, namely centrifugal stress (~240 MPa) and bending stress (~20 MPa). Assuming these stresses to be orthogonal and applying the Tresca Criterion  $\sigma_y/2 = (\sigma_1 - \sigma_2)$  for yielding, we find that the above two mentioned stresses acting in conjunction are insufficient to cause yielding.

However, once a crack/pit forms by silica impingement and is further elongated due to the operation of the chloride enhanced crevice attack mechanism, there is a significant stress concentration at the crack/eroded pit tip. The increase in stress is also brought about by a reduction in cross-section (due to the presence of a crack/eroded pit) and eventually the principal stresses at the crack/eroded pit tip are high enough to cause crack propagation catastrophically.

If the blades are kept clean and free of deposits and debris, crevice corrosion and pitting can be prevented or minimised.

## 5. Conclusions

- The blade material was as per specified grade of steel and there was no inhomogeneity regarding microstructure of the blade material.
- Throughout the blade surface deposits containing Si was detected. It is expected that the impingement of silica particles led to formation of pits.

- Several pits/grooves were found on the edges of the blades and presence of chloride salt in these pits was responsible for the initiation of crack by crevice corrosion.
- Calcium and potassium chlorides were found on the blade surface.
- The failure mode was intergranular type. In all probability, failure was due to corrosion-fatigue.
- The water chemistry should be checked properly and the silica and chloride level should be under control.

### **Acknowledgements**

The authors are grateful to Professor P. Ramachandra Rao, Director NML Jamshedpur for his kind permission to publish this manuscript.

### **References**

- [1] Mukhopadhyay NK, Ghosh Chowdhury S, Das G, Chattoraj I, Das SK, Bhattacharya DK. *Eng Failure Analysis* 1998;5(3):181.
- [2] ASM handbook, Vol. 1., ASM Metals Park (OH), 1993. p. 284.
- [3] Jones, DRH, *Engineering materials 3*, Pergamon Press, London; 1993, p.358.
- [4] Dieter GE. *Mechanical metallurgy*. McGraw-Hill Publishers; 1988. p. 373.
- [5] Levy AV. In: Srinivasan V, Vedula K, editors. *Corrosion and particle erosion at high temperature*. TMS; 1989. p. 207.
- [6] Levy, AV. *Solid particle erosion and erosion-corrosion of materials*. ASM International, 1995.
- [7] *Corrosion related failure in feed water heaters*, EPRI CS/NP-3743, Electric Power Research Institute, October 1984.
- [8] *Failure cause—feed water heaters*, EPRI CS-17776, Electric Power Research Institute, April 1981.
- [9] *Metals Handbook*, ASTM International, vol. 13, 9th ed. *Corrosion in fossil fuel power*. 1987., p. 999.